Geophysical Research Letters

RESEARCH LETTER
10.1029/2022GL102552

First Mapping of Monthly and Diurnal Climatology of Saharan Dust Layer Height Over the Atlantic Ocean From EPIC/DSCOVR in Deep Space

Zhendong Lu[1], Jun Wang[1,2], Xi Chen[2], Jing Zeng[2], Yi Wang[2,3], Xiaoguang Xu[4], Kenneth E. Christian[5,6], John E. Yorks[5], Edward P. Nowottnick[5], Jeffrey S. Reid[7], and Peng Xian[7]

[1]Interdisciplinary Graduate Program in Informatics, The University of Iowa, Iowa City, IA, USA, [2]Department of Chemical and Biochemical Engineering, Center for Global and Regional Environmental Research and Iowa Technology Institute, The University of Iowa, Iowa City, IA, USA, [3]Now at Hubei Key Laboratory of Regional Ecology and Environmental Change, School of Geography and Information Engineering, China University of Geosciences, Wuhan, China, [4]GESTAR-II and Department of Physics, University of Maryland Baltimore County, Baltimore, MD, USA, [5]NASA Goddard Space Flight Center, Greenbelt, MD, USA, [6]Earth System Science Interdisciplinary Center, University of Maryland, College Park, MD, USA, [7]U.S. Naval Research Laboratory, Monterey, CA, USA

Abstract The monthly and hourly climatology of Saharan dust layer height over the Atlantic, at a spatial resolution of ~10 km, is obtained for the first time, via a passive remote sensing technique. The technique is applied to multiple years of Earth Polychromatic Imaging Camera (EPIC) data collected at the Lagrange-1 point, generating a climate data record (CDR) of aerosol optical centroid height (AOCH). This CDR offers unprecedented spatial coverage and diurnal sampling compared to spaceborne lidars (CALIOP and CATS). Our results show high correspondence with CALIOP data in domain-averaged monthly variations and with CATS data in diurnal variations, respectively. A principal component analysis (PCA) reveals the dominant role of dust transport in regulating AOCH variation, whereas the impact of the boundary layer is less significant. MERRA-2 and satellite retrievals respectively display zero and 200–1,000 m of diurnal variation of AOCH, highlighting the uniqueness of EPIC AOCH CDR in constraining climate models.

Plain Language Summary The vertical distribution of atmospheric dust particles affects the Earth's radiative balance, air quality prediction, and remote sensing of greenhouse gases and aerosols but is poorly represented in model reanalysis, such as MERRA-2. In this study, the monthly mean heights of the Saharan dust plume are characterized based on a retrieval of Earth Polychromatic Imaging Camera (EPIC) measurements using 4 years of data. The unique position of the EPIC instrument at the Lagrange-1 point, between the Earth and the sun, enables the observation of the sunlit side of the Earth every 1–2 hr. From these observations, the hourly mean climatology of Saharan dust plume height can be calculated. We find that the EPIC-retrieved dust layer heights agree well with spaceborne lidar data. Our analysis shows that trans-Atlantic dust transport dominates the variability in the dust layer heights observed by EPIC. This study is among the first to demonstrate the strong synergy between the passive sensing featuring large spatial coverage and active sensing with detailed profiling for characterizing the diurnal variation of aerosol vertical distribution and processes as well as the need of such synergy for the climate modeling studies.

Key Points:

- Hourly and monthly climatology of Saharan dust layer height distribution over the ocean is first mapped from passive remote sensing (Earth Polychromatic Imaging Camera)
- The climatology agrees with that from spaceborne lidars and attests to the deficiency in model reanalysis of dust height diurnal change
- A combination of active and passive sensing techniques to study process for time-varying 3D aerosol distribution climatology

Supporting Information:

Supporting Information may be found in the online version of this article.

Correspondence to:

J. Wang,
jun-wang-1@uiowa.edu

Citation:

Lu, Z., Wang, J., Chen, X., Zeng, J., Wang, Y., Xu, X., et al. (2023). First mapping of monthly and diurnal climatology of Saharan dust layer height over the Atlantic Ocean from EPIC/DSCOVR in deep space. *Geophysical Research Letters*, *50*, e2022GL102552. https://doi.org/10.1029/2022GL102552

Received 22 JUN 2022
Accepted 22 JAN 2023

1. Introduction

Current atmospheric models have significant difficulties in simulating the vertical distribution of aerosols (Kipling et al., 2016; Koffi et al., 2016), especially for dust (D. Kim et al., 2014; O'Sullivan et al., 2020). The uncertainty of total column dust aerosol optical depth (AOD) in chemical transport models is generally within a factor of 2, but the deposition flux and surface concentration of dust that depend on the dust vertical distribution have the uncertainties of up to a factor of 10 (Huneeus et al., 2011). The dust vertical distribution regulates the regional dust radiative forcing and cloud process (Mishra et al., 2015; Zhang et al., 2013), ocean biogeochemistry and marine ecosystem productivity (Jickells et al., 2005; Ussher et al., 2013; Yu et al., 2019), soil nutrient balance (Das et al., 2013; Rizzolo et al., 2017; Yu, Chin, Yuan, et al., 2015), as well as air quality (Bozlaker et al., 2013; Prospero et al., 2014). Therefore, the observations of three-dimensional distribution of dust are necessary for evaluating, constraining, and improving the model simulations and thus to better understand the role of dust

in the environment and the climate system (Colarco et al., 2003; Huneeus et al., 2011; D. Kim et al., 2014; Nowottnick et al., 2010; Yu, Chin, Bian, et al., 2015).

Around 200 million tons of dust are transported from North Africa to the Atlantic every year (Yu, Chin, Bian, et al., 2015; Yu et al., 2019). However, the climatology of the diurnal variation of trans-Atlantic dust vertical distribution remains unclear due to the lack of observations. While ground or space-based lidar can provide observations of cloud and aerosol vertical distributions, they suffer from limited spatial coverage. The Cloud-Aerosol Lidar with Orthogonal Polarization (CALIOP) measurements (Winker et al., 2009) only cover 0.2% of the global surface area in its repeat cycle of 16 days (Kahn et al., 2008). The Cloud-Aerosol Transport System (CATS) onboard the International Space Station (ISS) featured a finer temporal resolution with a shorter revisit cycle (~3 days) and provided measurements at various local times, but its operation only lasted for less than 3 years (February 2015 to October 2017). While passive satellite remote sensing provides less information about the aerosol vertical distribution than active sensors, its larger spatial coverage provides a valuable tool to fill the spatial gap left by the relatively sparse lidar data. The techniques for passive remote sensing of aerosol vertical distribution include stereo photogrammetry (Nelson et al., 2013), polarization or radiance-only measurements in UV or deep blue channels (J. Lee et al., 2020; Wu et al., 2016), oxygen or oxygen-dimer absorption spectroscopy (Chimot et al., 2018; Xu et al., 2017, 2019) and infrared thermal techniques (Peyridieu et al., 2010; Vandenbussche et al., 2013). However, most passive satellite sensors with the capability of retrieving aerosol layer height (ALH) are located at sun-synchronous orbits, which can only provide the measurement once per day at a fixed local time, such as Tropospheric Monitoring Instrument (TROPOMI) (Chen et al., 2021; Nanda et al., 2019). The Geostationary Environment Monitoring Spectrometer (GEMS) can potentially offer hourly ALH retrievals over East Asia (J. Kim et al., 2020; M. Kim et al., 2018), but hourly operational ALH over other regions is not currently available. The NASA mission Tropospheric Emissions: Monitoring of Pollution (TEMPO) may retrieve the hourly ALH using oxygen B-band over North America in the coming one or 2 years (Chance et al., 2019; Xu et al., 2019; Zoogman et al., 2017). Previous studies mapping the climatology of trans-Atlantic dust vertical distribution from thermal infrared measurements of Atmospheric Infrared Sounder (AIRS) (Peyridieu et al., 2010; Pierangelo et al., 2004) and CALIOP data (Liu et al., 2008; Tsamalis et al., 2013; Yu et al., 2019) cannot probe the diurnal variations. Furthermore, infrared techniques are subject to uncertainties in the temperature and water vapor profiles used in the retrieval (Vandenbussche et al., 2013).

Here, we retrieved the dust plume height over tropical North Atlantic Ocean (TNAO) from June 2015 to June 2019 using Earth Polychromatic Imaging Camera (EPIC) measurements on the Deep Space Climate Observatory (DSCOVR) with an algorithm developed by Xu et al. (2017). A dust height climatology was developed and analyzed in relation to monthly variation, diurnal variation, and key processes contributing to their variability. We compare the monthly and hourly climatology of EPIC dust layer heights with those observed by the sun-synchronous CALIOP lidar, the high inclination CATS lidar (McGill et al., 2015; Yorks et al., 2016) and those represented in the MERRA-2 (Modern-Era Retrospective analysis for Research and Applications, Version 2) data set (Gelaro et al., 2017). This illustrates not only the seasonal variations of dust height from observations but allows for evaluation of the performance of MERRA-2 in representing the diurnal variations of the dust vertical distribution. Moreover, the natural variability of the CALIOP monthly aerosol vertical profiles is provided by an objective principal component analysis (PCA) method, which is used to verify that the variation of EPIC AOCH is mainly driven by dust transport.

2. Data Sets and Methods

2.1. Characterization of EPIC AOCH Climatology

The EPIC measurements enable us to derive the aerosol optical centroid height (AOCH) for the same location multiple times daily (Lu et al., 2021; Xu et al., 2017, 2019). Orbiting at Lagrange-1 point, the EPIC imager observes the sunlit Earth disk every 1–2 hr at 10 narrow channels from the ultraviolet to near-infrared, including the oxygen A (764 nm) and B (688 nm) bands (Marshak et al., 2018), which can be used to retrieve the hourly AOCH (Lu et al., 2021; Xu et al., 2017, 2019). Four years of EPIC level 1B data (version 3) from June 2015 to June 2019 are collected to retrieve the AOCH of trans-Atlantic dust plume. The spatial resolution of EPIC measurements is ~10 km at nadir and ~20 km at a viewing zenith angle of 60° (Marshak et al., 2018). For more details of the EPIC AOCH retrieval algorithm, please refer to the Supporting Information and Xu et al. (2017).

The EPIC level 1B data is aggregated to the uniform grid boxes of 0.1° × 0.1° before the retrieval for the convenience of calculating multi-year mean of the retrieval results. Because of the coarse resolution of EPIC, the cloud mask may omit the contamination of some thin and small subpixel clouds. To address this issue, we applied a 3 pixel × 3 pixel moving template over the preliminary retrievals and removed the central pixel if any pixels covered by the template have been identified as clouds by the preliminary cloud mask. This aggressive post-retrieval processing may incorrectly remove some clear pixels close to broken clouds but can help us minimize the cloud contamination. The missing of certain clear pixels does not harm our purpose of characterizing the multi-year AOCH climatology. The pixels with the sun glint angle less than 30° are removed (Levy et al., 2013). To guarantee the retrieval quality, the AOCH retrievals under any of the following conditions are removed: (a) solar zenith angle or viewing zenith angle greater than 70°; (b) retrieved AOD lower than 0.2. The AOD threshold also help us focus on the Saharan dust transport cases where the optical depths are higher (D. Kim et al., 2014; Yu, Chin, Bian, et al., 2015). To further remove the data outliers, only the AOCH retrievals between the 25th and 75th percentiles of each hour or month are used to characterize the climatology of dust AOCH. The pixels with number of valid retrievals lower than 30 for each hour or month are screened out. The monthly sample density map is shown in Figure S1 in Supporting Information S1.

2.2. AOCH From Lidars and MERRA-2

Because we are mapping the AOCH climatology, the aggregated monthly aerosol extinction profiles from CALIOP level 3 product rather than level 2 data are used. We collected 13 years (June 2006 to June 2019) of CALIOP level 3 data with a horizontal resolution of 2° × 5° and vertical resolution of 60 m (Winker et al., 2013). Since EPIC only observed the sunlit side of the Earth, only daytime CALIOP data are used. To compare with EPIC AOCH climatology, the CALIOP AOCH is calculated as an effective height weighted by the AOD at each vertical layer using the CALIOP monthly aerosol extinction vertical profiles as

$$\mathrm{AOCH}_{\mathrm{CALIOP}} = \frac{\sum_{i=1}^{n} \beta_{\mathrm{ext},i} \Delta Z_i Z_i}{\sum_{i=1}^{n} \beta_{\mathrm{ext},i} \Delta Z_i} \quad (1)$$

where $\beta_{\mathrm{ext},i}$ is 532 nm aerosol extinction coefficient at vertical level i with the altitude of Z_i, and ΔZ_i is the layer thickness of vertical layer i. To match the overpass time of CALIOP, only the EPIC data from 14:00 to 16:59 UTC are used in this comparison.

The same AOCH calculation, following Equation 1, is applied to the CATS measurements. CATS only provides the measurements at 1,064 nm, because it lost the 532 nm channel due to a laser-stabilization issue (Yorks et al., 2016). The 1,064 nm channel is more sensitive and suitable than 532 nm to detect the dust particles that have size larger than fine-mode smoke or anthropogenic particles (Yorks et al., 2016). Three years of CATS level 2 Operation Profile DP product with a vertical resolution of 60 m in the wet seasons (May–October) of 2015–2017 are used for the comparison with hourly climatology of EPIC AOCH. The CATS instrument operated on the ISS from February 2015 to October 2017, which enables collocated observations with EPIC (the same location at various local time) and promotes the studies of diurnal changes of clouds and aerosols (L. Lee et al., 2019; McGill et al., 2015; Noel et al., 2018; Nowottnick et al., 2022). In a previous study, EPIC and CATS agreed well in their characterization of the aerosol diurnal cycle for a Southeast Asian domain dominated by smoke and marine aerosols (Nowottnick et al., 2022). Because the sun glint angle is usually smaller than 30° at 11:00 and 12:00 local solar time (LT) in the wet season, the EPIC data at these times are discarded. The corresponding CATS data are also discarded for the comparison to EPIC.

We computed the climatology of diurnal AOCH in the wet season from the 3-hourly instantaneous MERRA-2 data following Equation 1. MERRA-2 data is generated with a horizontal resolution of 0.5° × 0.625° at 72 GEOS-5 model layers from surface to 0.01 hPa in a hybrid sigma-p coordinate (Gelaro et al., 2017). Equation 1 here is slightly different from eq. 3 in Xu et al. (2017) in that the altitude is weighted by optical depth rather than extinction coefficient in this study. This change has no impact for CALIOP and CATS data because they have a uniform vertical resolution of 60 m, but it affects the AOCH calculation from MERRA-2. The calculation of dust mass extinction efficiency is described in Supporting Information S1.

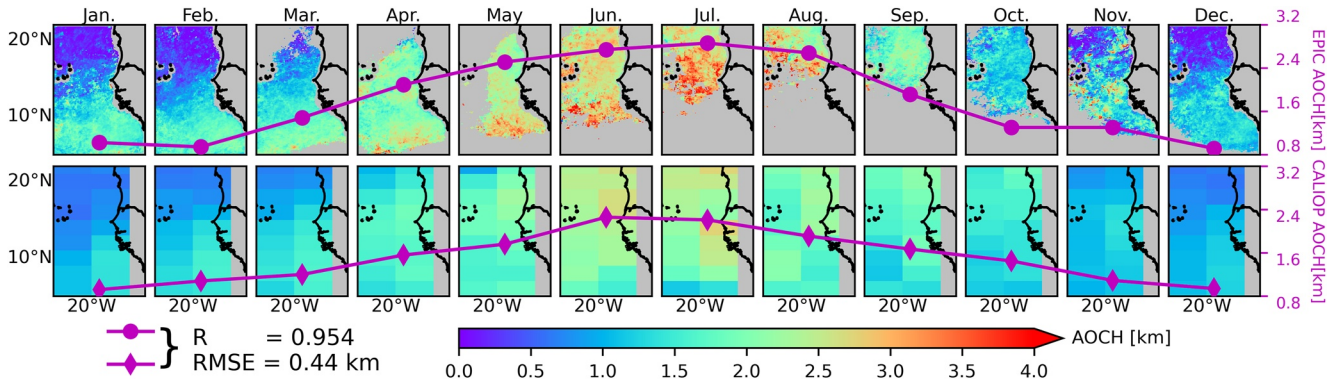

Figure 1. Comparison of monthly climatology of Earth Polychromatic Imaging Camera (EPIC) aerosol optical centroid height (AOCH) retrievals (top) and Cloud-Aerosol Lidar with Orthogonal Polarization (CALIOP) counterparts (bottom). Four years of EPIC data and 13 years of CALIOP data (daytime) are used for the comparison. The purple dot in each panel is the domain-averaged AOCH for each month in reference to the vertical coordinate on the right. The EPIC pixels with fewer valid retrievals due to the higher cloud fraction and lower sun glint angles in certain areas and seasons are screened out (gray areas over ocean in upper panels).

2.3. PCA of CALIOP Data

In the study area of TNAO, 13 years of CALIOP monthly data record reveal that dust particles are the dominant (>70%) contributor to the total AOD all year around, while smoke AOD only accounts for around 0.218%–2.50% of total AOD (Figure S2 in Supporting Information S1). Therefore, we hypothesize the annual cycle of AOCH monthly climatology in our study domain is primarily driven by dust transport. To objectively identify the orthogonal modes of variability in the aerosol vertical profiles and find the variation modes representing the dust transport, we conducted a PCA on the 13 years of monthly aerosol extinction profiles in daytime from CALIOP level 3 product over TNAO. PCA was used in the past studies to analyze the dominant mode in the aerosol vertical profiles measured by ground-based lidar (Chew et al., 2013; Reid et al., 2017), and the results reveal the altitude ranges where key processes occur (Reid et al., 2017). Each aerosol extinction profile involved in the PCA could be reconstructed by the following equation.

$$\beta_{\text{ext}}(z) = \sum_{i=1}^{n} P_i E_i(z) + \overline{\beta_{\text{ext}}}(z) \tag{2}$$

where $\beta_{\text{ext}}(z)$ is the aerosol extinction coefficient as a function of altitude z in a specific sample profile; $E_i(z)$ is the ith EOF (empirical orthogonal function, i.e., eigenvector); P_i is the PC (principal component) value of that sample profile in PC i; and $\overline{\beta_{\text{ext}}}(z)$ is the mean of all aerosol extinction profile samples. Here P_i could be considered as the weighting coefficient of EOF i for each aerosol profile anomaly. The correlation coefficients between the first 5 PCs and extinction profile samples at each vertical layer are computed to demonstrate at which altitude the variability of aerosol extinction can be best represented by each EOF (Reid et al., 2017).

3. Monthly Climatology of Saharan Dust Plume Heights

The multi-year monthly mean of EPIC AOCH over TNAO and the counterparts from 13 years of CALIOP level 3 monthly data are compared in Figure 1. The domain-averaged monthly AOCH is marked by purple dots in each panel in reference to the vertical coordinate on the right of Figure 1. The EPIC retrievals and CALIOP data share a similar monthly variation of AOCH with the correlation coefficient (R) of 0.95, root mean square error (RMSE) of 0.44 km, and mean bias error (MBE) of 0.31 km for the 12 domain-averaged monthly data points (see also Figure S3a in Supporting Information S1). Both EPIC and CALIOP data agree that the AOCH peaks in the summer months and is lowest in the wintertime, which is consistent with previous studies using CALIOP data (Liu et al., 2008; Yu et al., 2019) and thermal infrared measurements (Peyridieu et al., 2010; Pierangelo et al., 2004). MERRA-2 also captures the monthly variation of the Saharan dust AOCH (Figures S3b and S4 in Supporting Information S1). The EPIC and CALIOP AOCH also show that the Saharan dust transport belt shifts from the north in summer to the south in winter (see also Figure S2 in Supporting Information S1). This seasonal shift is caused by the movement of active dust sources in North Africa associated with the changes in small-scale near-surface wind fields and the annual shift of the Intertropical Convergence Zone (ITCZ) as well as the West African monsoon (Ben-Ami et al., 2012; Engelstaedter & Washington, 2007; Williams, 2008).

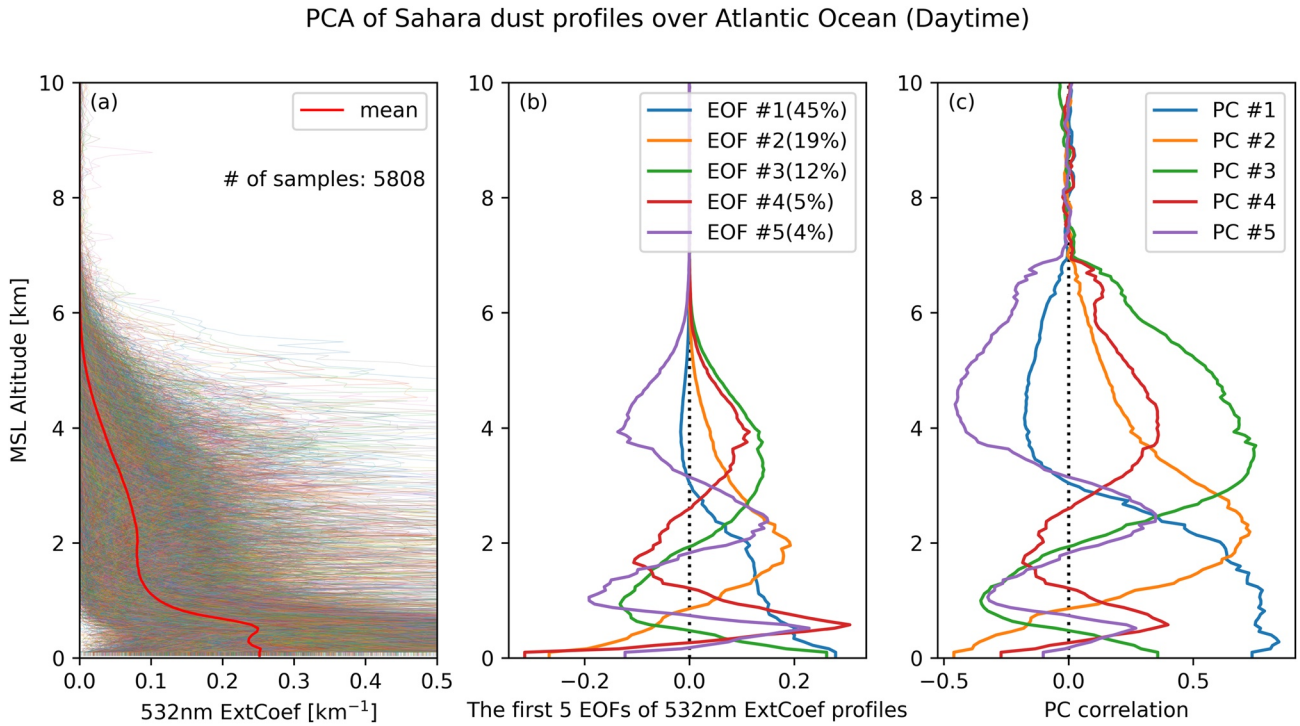

Figure 2. Principal component analysis (PCA) results for daytime aerosol extinction profiles over tropical North Atlantic Ocean using 13 years of Cloud-Aerosol Lidar with Orthogonal Polarization level 3 product (June 2006 to June 2019). (a) Original aerosol profile samples, (b) the first five empirical orthogonal function (EOF) modes, and (c) the correlation coefficients between the first five principal components and the original aerosol extinction coefficients in the sample data at each vertical layer. The vertical variance explained by each EOF is labeled in (b).

Figure 2 shows the first five EOF modes and the correlations between the first five PCs and the original extinction profiles at each vertical layer based on the PCA results. The vertical variance explained by each EOF is labeled in Figure 2b. The five major EOFs explain ~85% of total variability in the aerosol extinction profiles, and the first three EOFs account for ~76% of total variability. The altitude of each peak PC correlation value represents the height where the variability of aerosol extinction can be best explained by corresponding EOF (Reid et al., 2017). Figure 2c shows that EOF 1 best represents the marine boundary layer process such as boundary-layer mixing of sea salt below 2 km, while EOF 2 and 3 primarily account for the dust transport with vertical peaks at 2–4 km in the free troposphere given the elevated smoke is negligible in our domain (Figure S2 in Supporting Information S1).

We aggregated the first three PCs by month and compared them with the domain-averaged monthly EPIC AOCH (Figure 3). The sum of PC 2 and PC 3, which are the weights of the variations of dust transport in the mid-troposphere, has a high positive correlation with monthly EPIC AOCH with $R = 0.918$, while the PC 1 representing the weight of marine boundary layer variation is negatively correlated with EPIC AOCH with $R = -0.817$. It indicates that the EPIC AOCH is mostly controlled by the elevated dust transport in the free troposphere.

4. Hourly Climatology of Saharan Dust Plume Heights

Similar to L. Lee et al. (2019), we study the aerosol vertical distribution for two distinct seasons, that is, wet season (May–October) and dry season (November–April) over TNAO. The wet season features higher temperatures and precipitation than the dry season (Cropper & Hanna, 2014), which are associated with stronger convection and wet deposition. The 2-hr running average of EPIC AOCH retrievals for each hour are calculated to characterize the hourly climatology of dust layer height (Figure 4). The domain-averaged hourly climatology of AOCH from EPIC, CATS, and MERRA-2 are compared in Figure 4 for the wet season when the AOCH is more variable.

EPIC is the only passive satellite sensor that can currently provide the diurnal cycle of Saharan dust plume height. In dry season, the Saharan dust plumes rise slowly from early morning to the highest altitude at 13:00 LT

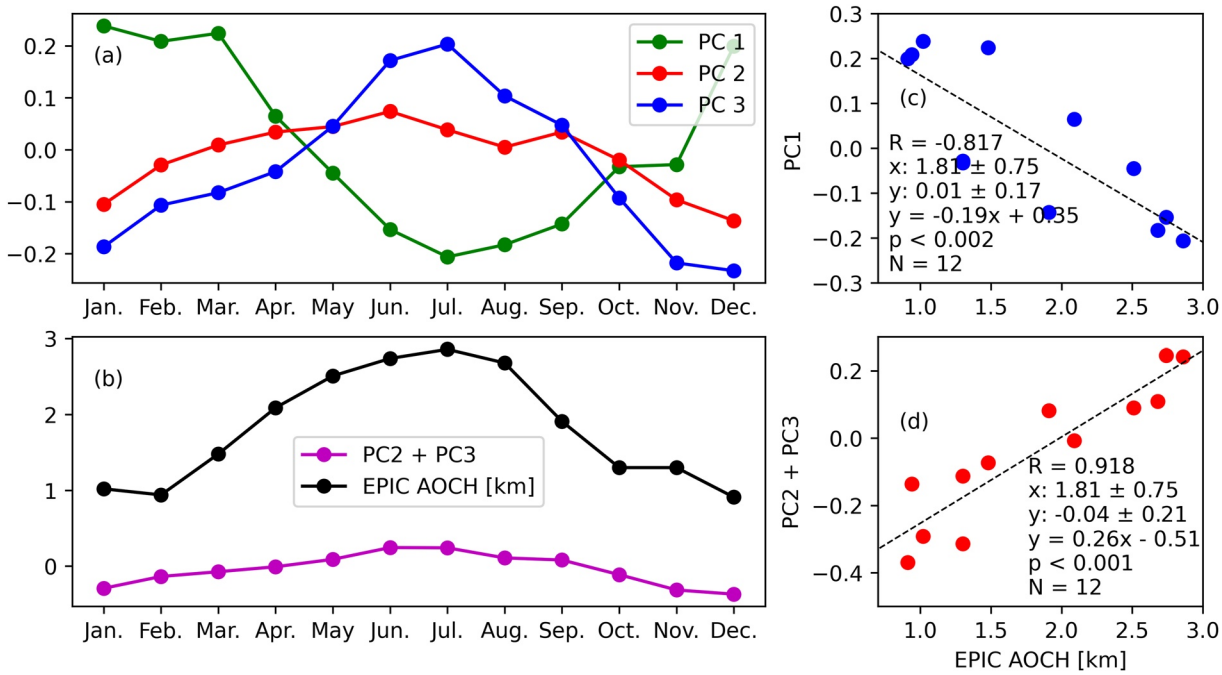

Figure 3. (a) The first three aggregated monthly principal components (PCs), (b) domain-averaged monthly Earth Polychromatic Imaging Camera (EPIC) aerosol optical centroid height (AOCH) and aggregated monthly PC 2 plus PC 3 and scatter plots of monthly EPIC AOCH versus (c) PC 1 and (d) PC 2 plus PC 3. The *R* value, mean and standard deviation of *x* and *y* axis, the fitted linear equation, and the total number of data points are labeled in (c) and (d).

by around 200 m, then descend through the afternoon hours. In contrast, dust layer height in wet season shows a larger diurnal variation in the EPIC AOCH data (Figure 4a). The dust layer height ascends rapidly by ~1 km from 07:00 to 10:00 LT, remains at a high altitude at 13:00 LT, and subsequently descends quickly in the afternoon. The CATS data is very sparse over the space and time compared to EPIC, and we only have 3 years of CATS data, which brings some uncertainties in the diurnal variation of CATS AOCH. However, we can still see the similar diurnal cycle of the AOCH from CATS and EPIC, both of which agree that the dust AOCH values are higher around noon and lower in the early morning and late afternoon, though there is a little drop from 9:00 to 10:00 LT for CATS AOCH (Figure 4b). L. Lee et al. (2019) also showed a rise of the aerosol layer in North Africa from early morning (6:00 LT) to noontime (12:00 LT) for the wet season using CATS data (see their Figure. 12), though they did not quantitatively calculate the AOCH and had a different domain and coarser temporal resolution than this study. We conjecture that this diurnal cycle of Saharan dust plume height results from the diurnal variation of solar heating that causes the thermal buoyancy to lift the dust layer and the diurnal evolution of the boundary layer. We also analyzed CALIOP data and found that AOCH from CALIOP in the study region is statistically significantly higher in the daytime than in the nighttime (results not shown), which supports our conjecture here. Further evaluation of this conjecture is complicated by the limited sampling of CALIOP data and the fixed overpassing time and can be the focus of future studies possible with intensive field campaigns and ground-based observation.

In comparison, the dust AOCH from MERRA-2 shows little diurnal variation, although they share the similar spatial pattern as EPIC (Figure S5 in Supporting Information S1). The lack of diurnal variation of AOCH in MERRA-2 may be associated with the lack of observational constraints for implementing diurnal boundary-layer mixing or thermal buoyancy in the model. We also evaluated the diurnal variation of the dust layer height from the 6-hourly NAAPS-RA (Navy Aerosol Analysis and Prediction System AOD reanalysis) data (Lynch et al., 2016). Similar to MERRA-2, the spatial distribution of Saharan dust height from NAAPS-RA is consistent with that of EPIC, but it is almost constant during the whole day including nighttime (Figure S6 in Supporting Information S1). Overall, from a climatological point of view, the results suggest that EPIC retrievals have potential to constrain model simulations of the diurnal variation of the dust vertical distribution. While more studies are needed, current models need improvement to accurately represent the diurnal variation of dust vertical distribution.

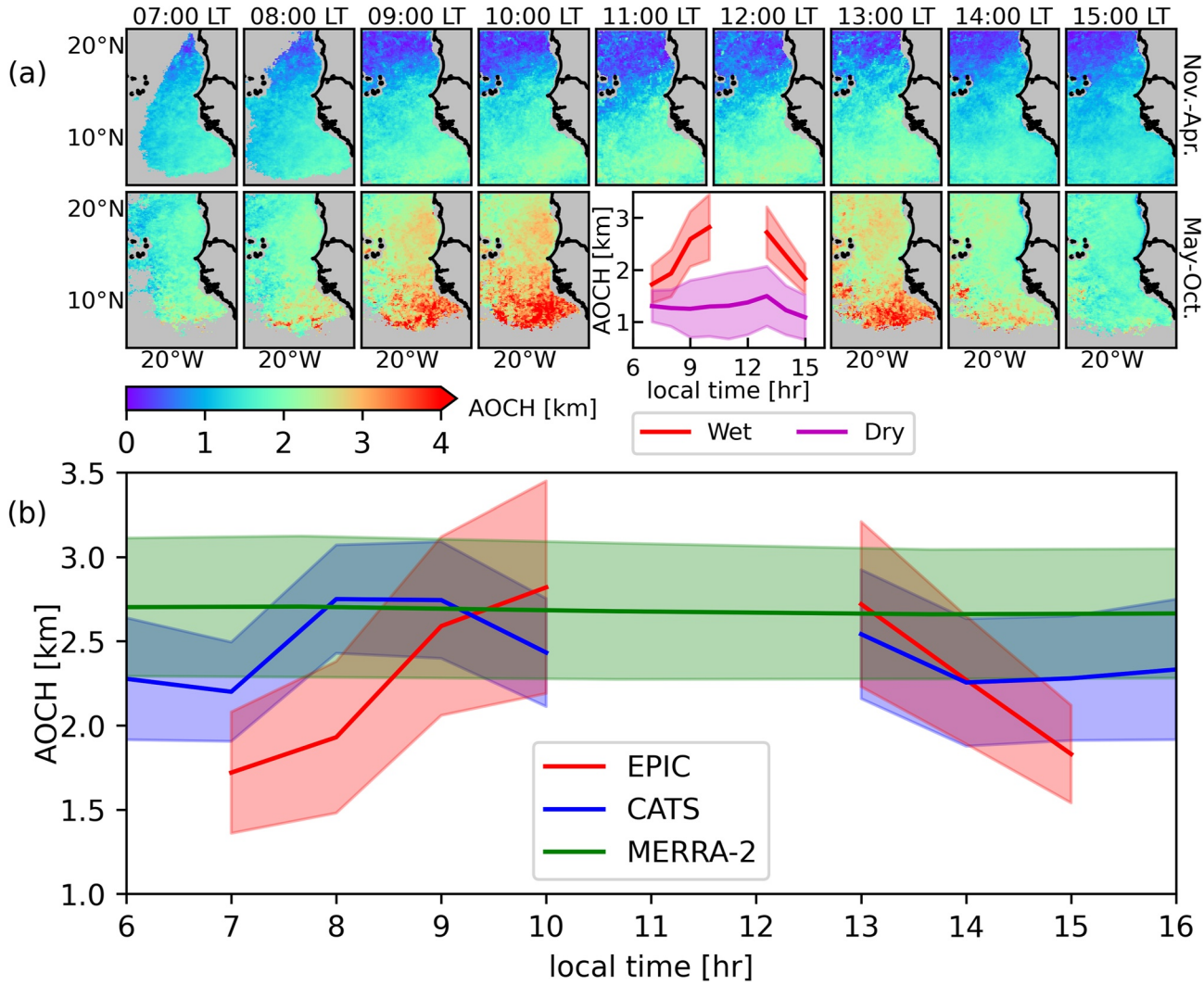

Figure 4. (a) The hourly climatology of Earth Polychromatic Imaging Camera (EPIC) aerosol optical centroid height (AOCH) by local time (LT) for dry season (first row, November–April) and wet season (second row, May–October). The domain-averaged hourly mean from dry and wet seasons are compared in the middle of second row. (b) The comparison of domain-averaged hourly climatology of EPIC AOCH in the wet season with the counterparts from CATS and MERRA-2. The EPIC and CATS data at 11:00 and 12:00 LT in the wet season are not shown due to the contamination of sun glint.

5. Summary

We retrieved the AOCH over the TNAO using 4 years of EPIC measurements and characterized the monthly and hourly climatology of the trans-Atlantic dust layer height. The monthly climatology of EPIC AOCH agrees well with CALIOP with an R value of 0.95 and RMSE of 0.44 km. The Saharan dust layer is highest in summer and lowest in wintertime, which is consistent with our current knowledge of the seasonal cycle of the Saharan dust vertical distribution (Liu et al., 2008; Peyridieu et al., 2010; Pierangelo et al., 2004). However, the CALIOP level 3 data has a coarse spatial resolution of $2° \times 5°$ and EPIC retrievals feature a much finer resolution of ~10 km. The PCA of aerosol extinction profiles indicates that the PC values that best represent the variability of Saharan dust transport, has a high positive R value of 0.918 with the EPIC monthly AOCH climatology. The weight of EOF 1 primarily accounting for the marine boundary layer process is negatively correlated with EPIC monthly AOCH. This indicates that the ascending of the ALH over TNAO in the summer and the annual variations are mainly due to the Saharan dust transport rather than the marine boundary layer process.

The characterization of the diurnal AOCH climatology over the TNAO is enabled by the unique Lagrange-1 point orbit of EPIC. In our domain, we found that Saharan dust plumes reach their peak height at local noon and their lowest height in the early morning and late afternoon. The diurnal cycle is more variable in the wet season

than in the dry season. From early morning to local noon, the EPIC AOCH ascends by ∼200 m in the dry season and ∼1 km in the wet season. The CATS data shows a similar diurnal variation in dust layer height as EPIC. In contrast, the diurnal AOCH from MERRA-2 (and NAAPS-RA) is almost constant throughout the day. While future studies are warranted to understand the reason for the model deficiency in simulating the AOCH diurnal climatology, the EPIC datasets of the diurnal variation of dust layer height may aid in constraining modeled dust vertical distributions, improving our understanding of dust environmental and climate effects. To statistically resolve the diurnal variation of aerosol vertical profile on regional and seasonal scales, future space-based missions should leverage the synergistic combination of active and passive sensors to provide vertically resolved estimate of aerosol loading with more spatial and temporal coverage.

Data Availability Statement

EPIC level 1B data are obtained from NASA Aura Validation Data Center (https://avdc.gsfc.nasa.gov/pub/DSCOVR/Level1b_v03/). EPIC level 2 AOCH data can be found at https://opendap.larc.nasa.gov/opendap/DSCOVR/EPIC/L2_AOCH_01/contents.html. CALIOP level 3 data are from https://asdc.larc.nasa.gov/data/CALIPSO/LID_L3_Tropospheric_APro_CloudFree-Standard-V4-20/. Earthdata registration is required for the access to the CALIOP level 3 data. CATS data are from https://cats.gsfc.nasa.gov/data/browse/. MERRA-2 data are from https://gmao.gsfc.nasa.gov/reanalysis/MERRA-2/data_access/. NAAPS-RA data can be found at https://usgodae.org/cgi-bin/datalist.pl?dset=nrl_naaps_reanalysis&summary=Go.

Acknowledgments
This work is supported by the NASA DSCOVR program (Grants 80NSSC19K1283 and 80NSSC22K0503) and NOAA (Grant NA21OAR4310249).

References

Ben-Ami, Y., Koren, I., Altaratz, O., Kostinski, A., & Lehahn, Y. (2012). Discernible rhythm in the spatio/temporal distributions of transatlantic dust. *Atmospheric Chemistry and Physics*, *12*(5), 2253–2262. https://doi.org/10.5194/acp-12-2253-2012

Bozlaker, A., Prospero, J. M., Fraser, M. P., & Chellam, S. (2013). Quantifying the contribution of long-range Saharan dust transport on particulate matter concentrations in Houston, Texas, using detailed elemental analysis. *Environmental Science & Technology*, *47*(18), 10179–10187. https://doi.org/10.1021/es4015663

Chance, K., Liu, X., Miller, C. C., Abad, G. G., Huang, G., Nowlan, C., et al. (2019). TEMPO green paper: Chemistry, physics, and meteorology experiments with the tropospheric emissions: Monitoring of pollution instrument. Paper presented at the Conference on Sensors, Systems, and Next-Generation Satellites XXIII.

Chen, X., Wang, J., Xu, X., Zhou, M., Zhang, H., Castro Garcia, L., et al. (2021). First retrieval of absorbing aerosol height over dark target using TROPOMI oxygen B band: Algorithm development and application for surface particulate matter estimates. *Remote Sensing of Environment*, *265*, 112674. https://doi.org/10.1016/j.rse.2021.112674

Chew, B. N., Campbell, J. R., Salinas, S. V., Chang, C. W., Reid, J. S., Welton, E. J., et al. (2013). Aerosol particle vertical distributions and optical properties over Singapore. *Atmospheric Environment*, *79*, 599–613. https://doi.org/10.1016/j.atmosenv.2013.06.026

Chimot, J., Veefkind, J. P., Vlemmix, T., & Levelt, P. F. (2018). Spatial distribution analysis of the OMI aerosol layer height: A pixel-by-pixel comparison to CALIOP observations. *Atmospheric Measurement Techniques*, *11*(4), 2257–2277. https://doi.org/10.5194/amt-11-2257-2018

Colarco, P. R., Toon, O. B., Reid, J. S., Livingston, J. M., Russell, P. B., Redemann, J., et al. (2003). Saharan dust transport to the Caribbean during PRIDE: 2. Transport, vertical profiles, and deposition in simulations of in situ and remote sensing observations. *Journal of Geophysical Research-Atmospheres*, *108*(D19), 8590. https://doi.org/10.1029/2002jd002659

Cropper, T. E., & Hanna, E. (2014). An analysis of the climate of Macaronesia, 1865-2012. *International Journal of Climatology*, *34*(3), 604–622. https://doi.org/10.1002/joc.3710

Das, R., Evan, A., & Lawrence, D. (2013). Contributions of long-distance dust transport to atmospheric P inputs in the Yucatan Peninsula. *Global Biogeochemical Cycles*, *27*(1), 167–175. https://doi.org/10.1029/2012gb004420

Engelstaedter, S., & Washington, R. (2007). Atmospheric controls on the annual cycle of North African dust. *Journal of Geophysical Research-Atmospheres*, *112*(D3), D03103. https://doi.org/10.1029/2006jd007195

Gelaro, R., McCarty, W., Suarez, M. J., Todling, R., Molod, A., Takacs, L., et al. (2017). The modern-era retrospective analysis for research and applications, version 2 (MERRA-2). *Journal of Climate*, *30*(14), 5419–5454. https://doi.org/10.1175/jcli-d-16-0758.1

Huneeus, N., Schulz, M., Balkanski, Y., Griesfeller, J., Prospero, J., Kinne, S., et al. (2011). Global dust model intercomparison in AeroCom phase I. *Atmospheric Chemistry and Physics*, *11*(15), 7781–7816. https://doi.org/10.5194/acp-11-7781-2011

Jickells, T. D., An, Z. S., Andersen, K. K., Baker, A. R., Bergametti, G., Brooks, N., et al. (2005). Global iron connections between desert dust, ocean biogeochemistry, and climate. *Science*, *308*(5718), 67–71. https://doi.org/10.1126/science.1105959

Kahn, R. A., Chen, Y., Nelson, D. L., Leung, F. Y., Li, Q. B., Diner, D. J., & Logan, J. A. (2008). Wildfire smoke injection heights: Two perspectives from space. *Geophysical Research Letters*, *35*(4), L04809. https://doi.org/10.1029/2007gl032165

Kim, D., Chin, M., Yu, H. B., Diehl, T., Tan, Q., Kahn, R. A., et al. (2014). Sources, sinks, and transatlantic transport of North African dust aerosol: A multimodel analysis and comparison with remote sensing data. *Journal of Geophysical Research-Atmospheres*, *119*(10), 6259–6277. https://doi.org/10.1002/2013jd021099

Kim, J., Jeong, U., Ahn, M. H., Kim, J. H., Park, R. J., Lee, H., et al. (2020). New era of air quality monitoring from space: Geostationary environment monitoring spectrometer (GEMS). *Bulletin of the American Meteorological Society*, *101*(1), E1–E22. https://doi.org/10.1175/bams-d-18-0013.1

Kim, M., Kim, J., Torres, O., Ahn, C., Kim, W., Jeong, U., et al. (2018). Optimal estimation-based algorithm to retrieve aerosol optical properties for GEMS measurements over Asia. *Remote Sensing*, *10*(2), 162. https://doi.org/10.3390/rs10020162

Kipling, Z., Stier, P., Johnson, C. E., Mann, G. W., Bellouin, N., Bauer, S. E., et al. (2016). What controls the vertical distribution of aerosol? Relationships between process sensitivity in HadGEM3–UKCA and inter-model variation from AeroCom Phase II. *Atmospheric Chemistry and Physics*, *16*(4), 2221–2241. https://doi.org/10.5194/acp-16-2221-2016

Koffi, B., Schulz, M., Breon, F. M., Dentener, F., Steensen, B. M., Griesfeller, J., et al. (2016). Evaluation of the aerosol vertical distribution in global aerosol models through comparison against CALIOP measurements: AeroCom phase II results. *Journal of Geophysical Research: Atmospheres*, *121*(12), 7254–7283. https://doi.org/10.1002/2015JD024639

Lee, J., Hsu, N. C., Sayer, A. M., Seftor, C. J., & Kim, W. V. (2020). Aerosol layer height with enhanced spectral coverage achieved by synergy between VIIRS and OMPS-NM measurements. *IEEE Geoscience and Remote Sensing Letters*, *18*(6), 1–5. https://doi.org/10.1109/lgrs.2020.2992099

Lee, L., Zhang, J. L., Reid, J. S., & Yorks, J. E. (2019). Investigation of CATS aerosol products and application toward global diurnal variation of aerosols. *Atmospheric Chemistry and Physics*, *19*(19), 12687–12707. https://doi.org/10.5194/acp-19-12687-2019

Levy, R. C., Mattoo, S., Munchak, L. A., Remer, L. A., Sayer, A. M., Patadia, F., & Hsu, N. C. (2013). The Collection 6 MODIS aerosol products over land and ocean. *Atmospheric Measurement Techniques*, *6*(11), 2989–3034. https://doi.org/10.5194/amt-6-2989-2013

Liu, D., Wang, Z., Liu, Z. Y., Winker, D., & Trepte, C. (2008). A height resolved global view of dust aerosols from the first year CALIPSO Lidar measurements. *Journal of Geophysical Research-Atmospheres*, *113*(D16), D16214. https://doi.org/10.1029/2007jd009776

Lu, Z., Wang, J., Xu, X., Chen, X., Kondragunta, S., Torres, O., et al. (2021). Hourly mapping of the layer height of thick smoke plumes over the Western U.S. In 2020 Severe Fire season. *Frontiers in Remote Sensing*, *2*, 766628. https://doi.org/10.3389/frsen.2021.766628

Lynch, P., Reid, J. S., Westphal, D. L., Zhang, J. L., Hogan, T. F., Hyer, E. J., et al. (2016). An 11-year global gridded aerosol optical thickness reanalysis (v1.0) for atmospheric and climate sciences. *Geoscientific Model Development*, *9*(4), 1489–1522. https://doi.org/10.5194/gmd-9-1489-2016

Marshak, A., Herman, J., Szabo, A., Blank, K., Carn, S., Cede, A., et al. (2018). Earth observations from DSCOVR EPIC instrument. *Bulletin of the American Meteorological Society*, *99*(9), 1829–1850. https://doi.org/10.1175/bams-d-17-0223.1

McGill, M. J., Yorks, J. E., Scott, V. S., Kupchock, A. W., & Selmer, P. A. (2015). The cloud-aerosol transport system (CATS): A technology demonstration on the International Space Station. Paper presented at the Conference on Lidar Remote Sensing for Environmental Monitoring XV.

Mishra, A. K., Koren, I., & Rudich, Y. (2015). Effect of aerosol vertical distribution on aerosol-radiation interaction: A theoretical prospect. *Heliyon*, *1*(2), e00036. https://doi.org/10.1016/j.heliyon.2015.e00036

Nanda, S., de Graaf, M., Veefkind, J. P., ter Linden, M., Sneep, M., de Haan, J., & Levelt, P. F. (2019). A neural network radiative transfer model approach applied to the Tropospheric Monitoring Instrument aerosol height algorithm. *Atmospheric Measurement Techniques*, *12*(12), 6619–6634. https://doi.org/10.5194/amt-12-6619-2019

Nelson, D. L., Garay, M. J., Kahn, R. A., & Dunst, B. A. (2013). Stereoscopic height and wind retrievals for aerosol plumes with the MISR INteractive eXplorer (MINX). *Remote Sensing*, *5*(9), 4593–4628. https://doi.org/10.3390/rs5094593

Noel, V., Chepfer, H., Chiriaco, M., & Yorks, J. (2018). The diurnal cycle of cloud profiles over land and ocean between 51 degrees S and 51 degrees N, seen by the CATS spaceborne Lidar from the International Space Station. *Atmospheric Chemistry and Physics*, *18*(13), 9457–9473. https://doi.org/10.5194/acp-18-9457-2018

Nowottnick, E., Christian, K. E., Yorks, J. E., McGill, M. J., Midzak, N., Selmer, P. A., et al. (2022). Aerosol detection from the cloud-aerosol transport system on the International Space Station: Algorithm overview and implications for diurnal sampling. *Atmosphere*, *13*(9), 1439. https://doi.org/10.3390/atmos13091439

Nowottnick, E., Colarco, P., Ferrare, R., Chen, G., Ismail, S., Anderson, B., & Browell, E. (2010). Online simulations of mineral dust aerosol distributions: Comparisons to NAMMA observations and sensitivity to dust emission parameterization. *Journal of Geophysical Research-Atmospheres*, *115*(D3), D03202. https://doi.org/10.1029/2009jd012692

O'Sullivan, D., Marenco, F., Ryder, C. L., Pradhan, Y., Kipling, Z., Ben, J., et al. (2020). Models transport Saharan dust too low in the atmosphere: A comparison of the MetUM and CAMS forecasts with observations. *Atmospheric Chemistry and Physics*, *20*(21), 12955–12982. https://doi.org/10.5194/acp-20-12955-2020

Peyridieu, S., Chedin, A., Tanre, D., Capelle, V., Pierangelo, C., Lamquin, N., & Armante, R. (2010). Saharan dust infrared optical depth and altitude retrieved from AIRS: A focus over North Atlantic – Comparison to MODIS and CALIPSO. *Atmospheric Chemistry and Physics*, *10*(4), 1953–1967. https://doi.org/10.5194/acp-10-1953-2010

Pierangelo, C., Chedin, A., Heilliette, S., Jacquinet-Husson, N., & Armante, R. (2004). Dust altitude and infrared optical depth from AIRS. *Atmospheric Chemistry and Physics*, *4*(7), 1813–1822. https://doi.org/10.5194/acp-4-1813-2004

Prospero, J. M., Collard, F.-X., Molinié, J., & Jeannot, A. (2014). Characterizing the annual cycle of African dust transport to the Caribbean Basin and South America and its impact on the environment and air quality. *Global Biogeochemical Cycles*, *28*(7), 757–773. https://doi.org/10.1002/2013GB004802

Reid, J. S., Kuehn, R. E., Holz, R. E., Eloranta, E. W., Kaku, K. C., Kuang, S., et al. (2017). Ground-based high spectral resolution Lidar observation of aerosol vertical distribution in the summertime Southeast United States. *Journal of Geophysical Research: Atmospheres*, *122*(5), 2970–3004. https://doi.org/10.1002/2016jd025798

Rizzolo, J. A., Barbosa, C. G. G., Borillo, G. C., Godoi, A. F. L., Souza, R. A. F., Andreoli, R. V., et al. (2017). Soluble iron nutrients in Saharan dust over the central Amazon rainforest. *Atmospheric Chemistry and Physics*, *17*(4), 2673–2687. https://doi.org/10.5194/acp-17-2673-2017

Tsamalis, C., Chedin, A., Pelon, J., & Capelle, V. (2013). The seasonal vertical distribution of the Saharan Air Layer and its modulation by the wind. *Atmospheric Chemistry and Physics*, *13*(22), 11235–11257. https://doi.org/10.5194/acp-13-11235-2013

Ussher, S. J., Achterberg, E. P., Powell, C., Baker, A. R., Jickells, T. D., Torres, R., & Worsfold, P. J. (2013). Impact of atmospheric deposition on the contrasting iron biogeochemistry of the North and South Atlantic Ocean. *Global Biogeochemical Cycles*, *27*(4), 1096–1107. https://doi.org/10.1002/gbc.20056

Vandenbussche, S., Kochenova, S., Vandaele, A. C., Kumps, N., & De Maziere, M. (2013). Retrieval of desert dust aerosol vertical profiles from IASI measurements in the TIR atmospheric window. *Atmospheric Measurement Techniques*, *6*(10), 2577–2591. https://doi.org/10.5194/amt-6-2577-2013

Williams, E. R. (2008). Comment on "Atmospheric controls on the annual cycle of North African dust" by S. Engelstaedter and R. Washington. *Journal of Geophysical Research-Atmospheres*, *113*(D23), D23109. https://doi.org/10.1029/2008jd009930

Winker, D. M., Tackett, J. L., Getzewich, B. J., Liu, Z., Vaughan, M. A., & Rogers, R. R. (2013). The global 3-D distribution of tropospheric aerosols as characterized by CALIOP. *Atmospheric Chemistry and Physics*, *13*(6), 3345–3361. https://doi.org/10.5194/acp-13-3345-2013

Winker, D. M., Vaughan, M. A., Omar, A., Hu, Y. X., Powell, K. A., Liu, Z. Y., et al. (2009). Overview of the CALIPSO mission and CALIOP data processing algorithms. *Journal of Atmospheric and Oceanic Technology*, *26*(11), 2310–2323. https://doi.org/10.1175/2009jtecha1281.1

Wu, L., Hasekamp, O., van Diedenhoven, B., Cairns, B., Yorks, J. E., & Chowdhary, J. (2016). Passive remote sensing of aerosol layer height using near-UV multiangle polarization measurements. *Geophysical Research Letters*, *43*(16), 8783–8790. https://doi.org/10.1002/2016GL069848

Xu, X., Wang, J., Wang, Y., Zeng, J., Torres, O., Reid, J. S., et al. (2019). Detecting layer height of smoke aerosols over vegetated land and water surfaces via oxygen absorption bands: Hourly results from EPIC/DSCOVR in deep space. *Atmospheric Measurement Techniques*, *12*(6), 3269–3288. https://doi.org/10.5194/amt-12-3269-2019

Xu, X., Wang, J., Wang, Y., Zeng, J., Torres, O., Yang, Y., et al. (2017). Passive remote sensing of altitude and optical depth of dust plumes using the oxygen A and B bands: First results from EPIC/DSCOVR at Lagrange-1 point. *Geophysical Research Letters*, *44*(14), 7544–7554. https://doi.org/10.1002/2017gl073939

Yorks, J. E., McGill, M. J., Palm, S. P., Hlavka, D. L., Selmer, P. A., Nowottnick, E. P., et al. (2016). An overview of the CATS level 1 processing algorithms and data products. *Geophysical Research Letters*, *43*(9), 4632–4639. https://doi.org/10.1002/2016GL068006

Yu, H., Chin, M., Bian, H. S., Yuan, T. L., Prospero, J. M., Omar, A. H., et al. (2015). Quantification of trans-Atlantic dust transport from seven-year (2007-2013) record of CALIPSO lidar measurements. *Remote Sensing of Environment*, *159*, 232–249. https://doi.org/10.1016/j.rse.2014.12.010

Yu, H., Chin, M., Yuan, T. L., Bian, H. S., Remer, L. A., Prospero, J. M., et al. (2015). The fertilizing role of African dust in the Amazon rainforest: A first multiyear assessment based on data from Cloud-Aerosol Lidar and Infrared Pathfinder Satellite Observations. *Geophysical Research Letters*, *42*(6), 1984–1991. https://doi.org/10.1002/2015gl063040

Yu, H., Tan, Q., Chin, M., Remer, L. A., Kahn, R. A., Bian, H., et al. (2019). Estimates of African dust deposition along the trans-Atlantic transit using the Decadelong record of aerosol measurements from CALIOP, MODIS, MISR, and IASI. *Journal of Geophysical Research: Atmospheres*, *124*(14), 7975–7996. https://doi.org/10.1029/2019JD030574

Zhang, L., Li, Q. B., Gu, Y., Liou, K. N., & Meland, B. (2013). Dust vertical profile impact on global radiative forcing estimation using a coupled chemical-transport-radiative-transfer model. *Atmospheric Chemistry and Physics*, *13*(14), 7097–7114. https://doi.org/10.5194/acp-13-7097-2013

Zoogman, P., Liu, X., Suleiman, R. M., Pennington, W. F., Flittner, D. E., Al-Saadi, J. A., et al. (2017). Tropospheric emissions: Monitoring of pollution (TEMPO). *Journal of Quantitative Spectroscopy & Radiative Transfer*, *186*, 17–39. https://doi.org/10.1016/j.jqsrt.2016.05.008

References From the Supporting Information

Colarco, P. R., da Silva, A., Chin, M., & Diehl, T. (2010). Online simulations of global aerosol distributions in the NASA GEOS-4 model and comparisons to satellite and ground-based aerosol optical depth. *Journal of Geophysical Research*, *115*(D14), D14207. https://doi.org/10.1029/2009jd012820

Colarco, P. R., Nowottnick, E. P., Randles, C. A., Yi, B. Q., Yang, P., Kim, K. M., et al. (2014). Impact of radiatively interactive dust aerosols in the NASA GEOS-5 climate model: Sensitivity to dust particle shape and refractive index. *Journal of Geophysical Research-Atmospheres*, *119*(2), 753–786. https://doi.org/10.1002/2013jd020046

Spurr, R., & Christi, M. (2014). On the generation of atmospheric property Jacobians from the (V)LIDORT linearized radiative transfer models. *Journal of Quantitative Spectroscopy & Radiative Transfer*, *142*, 109–115. https://doi.org/10.1016/j.jqsrt.2014.03.011